JGR

RESEARCH ARTICLE

Key Points:
- We developed a method to identify TGFs with no lower limit on fluence
- The fraction of strong in-cloud lightning that produces TGFs is estimated to be around 1 in 100
- Dim TGFs are likely rarer than expected from extrapolation of the known rate of brighter TGFs

Correspondence to:
S. A. Cummer,
cummer@duke.edu

A lightning-based search for nearby observationally dim terrestrial gamma ray flashes

L. E. McTague[1], S. A. Cummer[1], M. S. Briggs[2], V. Connaughton[2], M. Stanbro[2], and G. Fitzpatrick[3]

[1]Department of Electrical and Computer Engineering, Duke University, Durham, North Carolina, USA, [2]CSPAR, University of Alabama in Huntsville, Huntsville, Alabama, USA, [3]School of Physics, University College Dublin, Dublin, Ireland

Abstract Current space-based observations of terrestrial gamma ray flashes (TGFs) are capable of identifying only TGFs that exceed a lower brightness threshold. Observationally, dim TGFs that fall below this threshold are consequently difficult to find using photon-only search algorithms. Such TGFs are a potentially important part of the overall global TGF rate, and information on their occurrence rate would give important insight into TGF generation mechanisms. We describe and implement a lightning-based search for TGFs that uses the location and time of National Lightning Detection Network reported positive polarity, in-cloud (+IC) discharges of the type known to be directly associated with TGFs. These events identify a 200 μs search window when any associated TGF photons would have been detected. We show that this approach can detect TGFs without requiring a lower threshold on the detected photon brightness of the event, and thus is capable, in principle, of finding a population of weak TGFs. We find that TGFs occur at a rate between 1 in 40 and 1 in 500 of in-cloud lightning events that meet our study's criteria. The distribution of gamma ray counts in the search windows exhibits a statistically significant lack of nearby dim TGFs below the GBM search threshold. The data favor a brightness distribution in which nearby observationally dim TGFs are rare.

1. Introduction

Terrestrial gamma ray flashes (TGFs) are submillisecond bursts of intense gamma radiation that were first reported in the early 1990s by *Fishman et al.* [1994]. It is generally agreed upon that the relativistic runaway electron avalanche (RREA) process is the main source of TGFs [*Wilson*, 1925; *Gurevich et al.*, 1992]. RREA is the process by which electrons are accelerated in Earth's atmosphere by an electric field, ionize molecules in the atmosphere, and generate more relativistic electrons which undergo avalanche multiplication [*Gurevich et al.*, 1992] and scattering. This process is heavily dependent upon an injection of seed electrons to actually produce a TGF [*Dwyer*, 2007, 2008]. There are presently two possible mechanisms that produce TGFs: (1) relativistic feedback associated with large ambient fields [*Dwyer*, 2003, 2007, 2008] and (2) lightning leaders, which are associated with localized fields [*Moss et al.*, 2006; *Chanrion and Neubert*, 2010; *Dwyer*, 2004; *Carlson et al.*, 2010; *Celestin and Pasko*, 2011].

In recent years, the occurrence rate of TGFs has been one of their many important characteristics that has been studied in-depth by researchers around the world. They have found that it is crucial to look into two key factors that may affect the worldwide TGF rate: how many TGFs are presently being estimated to occur and what fraction of lightning may be TGF producing.

Most present estimates of total TGF rate vary between 1100 and 1400 TGFs/d worldwide [*Tierney et al.*, 2013; *Briggs et al.*, 2013; *Carlson et al.*, 2011]. Approximations of 1100 TGFs/d [*Briggs et al.*, 2013] and 1200 TGFs/d [*Tierney et al.*, 2013] were computed based solely on the number of TGFs found above instrument brightness thresholds set in place after satellite observations, which was extrapolated to determine a worldwide TGF occurrence rate. *Briggs et al.* [2013] utilized the Lightning Imaging Sensor (LIS) combined with observations by the Fermi Gamma ray Burst Monitor (GBM) and compensated for the regional dependency of the overall TGF rate. *Tierney et al.* [2013] integrated a power law distribution of TGFs generated using observations by GBM that were corrected for instrumental effects, such as detector dead time and pulse pile up, but does not consider the geographic dependency of TGF production. Both of these estimates constrain TGFs based on the brightness threshold employed by GBM, which introduces the question of whether or not there are TGFs that occur below this threshold. *Carlson et al.* [2011], on the other hand, determined the worldwide TGF

occurrence rate by comparing GBM observations of both terrestrial electron beams and TGFs. *Carlson et al.* [2011] estimated that up to 1400 TGFs may occur per day and does not directly constrain TGFs based on an overall brightness limit.

Far exceeding the estimates made by *Briggs et al.* [2013], *Tierney et al.* [2013], and *Carlson et al.* [2011] is the one computed by *Østgaard et al.* [2012] of approximately 50,000 TGFs occurring per day worldwide. This TGF rate is much higher than the others because it was found by lowering the detection threshold of the Reuven Ramaty High Energy Solar Spectroscopic Imager (RHESSI) to 1/100th of RHESSI's (1/50th of GBM's) brightness threshold based on aircraft observations from the Airborne Detector for Energetic Lightning Emissions (ADELE) [*Østgaard et al.*, 2012; *Smith et al.*, 2011a, 2011b]. In doing so, *Østgaard et al.* [2012] determined the number of TGFs that could be detected by RHESSI if the brightness limit (cutoff in the known TGF fluence power law) were lowered. This number of hypothetical TGFs was then used to determine the total number of TGFs that could hypothetically be detected by RHESSI per day and per year. It is also important to note that the 50,000 TGFs/d estimate also encompassed a larger area due to RHESSI's orbit which covers ±38°latitude [*Østgaard et al.*, 2012].

The fraction of lightning that may be TGF producing has also been widely studied, especially as it pertains to overall TGF occurrence rate. It is well established that at least many (but perhaps not all) TGFs occur in association with the initial upward movement of positive polarity in-cloud (+IC) lightning leaders that move negative charge upward [*Stanley et al.*, 2006; *Lu et al.*, 2010; *Shao et al.*, 2010]. *Briggs et al.* [2013] used LIS to approximate that 1 in 2600 lightning discharges produces TGFs. The 2600 lightning discharges are likely to include cloud-to-ground discharges (CGs) in addition to ICs because LIS observes all types of lightning. In addition, the aircraft-based search for TGFs using ADELE detected 1 TGF in 1213 flashes, some of which were likely CGs [*Smith et al.*, 2011a, 2011b]. On the contrary, *Østgaard et al.* [2012] assert that TGFs are produced by roughly 2% of all IC lightning.

The previous work done to estimate both the number of TGFs that occur worldwide and the fraction of lightning that produces them form the basis of the underlying question of this paper, namely, are there TGFs that exist below current TGF detection thresholds used by space-based instruments?

The term "observationally dim" refers to TGFs that could be

1. intrinsically dim, that is, they occur at average TGF altitudes, but have a lower number of total gamma rays;
2. low altitude, but have average TGF brightness; or
3. far away from detectors, but have average brightness at their source [*Carlson et al.*, 2012].

This study is only focused on the first two classes of TGFs, because these two classes of TGFs are so far unobserved and knowing how frequent TGFs in these classes occur would be scientifically valuable. The third class cited above, namely, TGFs that are far from detectors but are otherwise similar in intensity and altitude to known TGFs, are less interesting because we know they occur. They are not above threshold simply due to distance and propagation effects and would be detected if the spacecraft were located closer. On the contrary, this study seeks to find events that are not presently detectable when they are within the optimum efficiency region of space-based instruments or when such instruments are directly overhead. To ensure that this study only searches for events like this, we intentionally employ a distance range limit to compile a data set of events that are within the region of optimum detector efficiency according to the spacecraft, which is discussed further in section 3. Based on the goal of this study, we use the term "nearby observationally dim" (NOD) as the term for TGFs that are not detected with peak current greater than 15 kA (according to the National Lightning Detection Network, discussed further in section 3) and that are also within 400 km of Fermi's footprint. These events are therefore identified as being intrinsically weak or intrinsically average/bright but deep in the atmosphere. The nearby observationally dim TGFs described above will be referred to as NOD-TGFs in the remainder of this paper.

To determine the existence of NOD-TGFs, we first perform a targeted search by combining +IC events as detected by the National Lightning Detection Network (NLDN), GBM gamma ray count data, and ground-based lightning sensor measurements. A timing computation that compensates for light travel time is used to determine the source time of each event and the time in which the NOD-TGF's photons would have reached GBM, had they indeed been the result of an NOD-TGF. Each event's corresponding sferic is examined to determine if the signal is +IC-like, and therefore TGF-like because the sferics that are the direct measurement of a TGF often look similar to those of +ICs in ground-based radio data [*Connaughton et al.*, 2010;

Cummer et al., 2011; *Dwyer and Cummer*, 2013]. Because of this, the term "TGF-like" will refer to any +IC-like event found during this study. The TGF-like events are combined with GBM gamma ray counts that are detected within ±100 μs of the proposed Fermi peak time. These TGF-like events' counts are then statistically analyzed for any possible existence of NOD-TGFs. The results of this statistical analysis show that the majority of the events found during this search procedure are not TGFs and that the probability of TGF occurrence is between 1 in 500 and 1 in 40 in-cloud events. In addition, evidence is found that supports the existence of a significant drop in TGF frequency, relative to known power laws, for TGFs below current detection thresholds. This indicates that NOD-TGFs may be rarer than expected.

2. Data and Measurements

Each step of this search procedure relies heavily on the following three key facts that are based on what is already understood about TGFs:

1. Direct measurements of TGFs that have been linked with NLDN-located events are reported as +IC discharges with moderate to high peak current [*Lu et al.*, 2011; *Cummer et al.*, 2011].
2. At least some TGFs have been found to occur simultaneously with strong, low-frequency (LF, 3–300 kHz) radio emissions [*Cummer et al.*, 2011; *Connaughton et al.*, 2010; *Dwyer and Cummer*, 2013].
3. TGFs are produced during the initial upward leader propagation of +IC discharges [*Stanley et al.*, 2006; *Lu et al.*, 2010; *Shao et al.*, 2010].

These three facts enable us to identify potential NOD-TGFs through NLDN-reported +IC events that are sufficiently close to the footprint of Fermi and that are consistent with having been produced during early stage IC leader development. NLDN provides the discharge type and polarity of each event, the time of each event in milliseconds, each event's location (within a 50% error ellipse), and the peak current of each event in kiloamperes. More information about NLDN can be found in *Cummins et al.* [1998, 2009].

LF radio emissions provide a way to determine the time in which the event's photons would have reached a detecting satellite, had the event in question been an NOD-TGF. The ground-based, LF sensors are also crucial to this study because they provide a way to exploit the assumed relationship between LF radio data and TGFs in a way that cannot be done using satellite and NLDN data alone. Two identical LF sensors located at Duke University (Duke) and the Florida Institute of Technology (FIT) are used during this study. They each consist of two orthogonal magnetic field induction coils that measure dB/dt and use a 1 MHz GPS-synchronized sampling clock, which provides timing accuracy to ±2 μs [*Cummer et al.*, 2011].

Since satellites in low-Earth orbit are able to observe TGFs it is only natural that satellite instruments are the primary space-based detectors of TGFs at this point in time. These satellites include RHESSI, Astro-Rivelatore Gamma a Immagini Leggero (AGILE), and the Fermi Gamma ray Space Telescope. While any of these satellites' instruments could be used, as they all provide gamma ray photon data, this research will utilize the Gamma ray Burst Monitor (GBM) aboard the Fermi Gamma ray Space Telescope because it provides continuous, time-tagged event data logging with a higher inclination than AGILE and a higher TGF detection rate and sensitivity than RHESSI [*Fuschino et al.*, 2011; *Briggs et al.*, 2013; *Østgaard et al.*, 2012].

GBM's original method for onboard TGF detection uses triggering software that waits for significant increases in detected photons before it begins logging data [*Briggs et al.*, 2013]. As an additional method of detection, the Fermi GBM team also performs an offline ground search to identify additional TGFs that were not detected during the triggered search [*Briggs et al.*, 2013]. This offline ground search is based on continuous, time-tagged data with microsecond timing resolution that became available starting in 2010 [*Briggs et al.*, 2013]. The data recorded therein will be used during this study, because it provides continuous data when Fermi is passing over areas that are also visible to the Duke and FIT LF sensors as well as NLDN. The region where the events in this study occurred spans the Gulf of Mexico to the Caribbean, within range of both LF and NLDN sensors, as well as part of Fermi's orbit.

GBM uses two bismuth germinate (BGO) scintillators to observe photons with an energy range of 200 keV to ~40 MeV with an effective area range of 160 to 200 cm^2 [*Briggs et al.*, 2013]. The threshold presently used to identify TGF candidates in the GBM continuous time-tagged event data is at least four counts in each BGO detector, eight counts total [*Briggs et al.*, 2013]. The remaining 12 scintillators onboard GBM are sodium iodide (NaI) with an observable energy range of ~8 keV to ~1 MeV and effective area of 100 cm^2 [*Briggs et al.*, 2013]. These can be used, in conjunction with the BGO detectors, to potentially identify TGFs [*Briggs et al.*, 2013].

However, the counts used in the search will refer to BGO-detected gamma rays because of the BGO detectors' larger energy range and effective area.

3. The NLDN-Based Search Procedure

The procedure begins through compiling a list of high-to-moderate peak current ($I_{pk} \geq 15$ kA) +IC lightning events detected by NLDN. A peak current threshold was imposed primarily to keep the data set a manageable size. Limiting the number of non-TGF noise events is also important for this study because it will increase our sensitivity to nearby observationally dim TGFs. A data set 10 times the size of the one used during this analysis, which would be expected if we included events with peak current less than 15 kA, will significantly increase our noise threshold.

This peak current threshold does introduce a bias into our data set and could exclude some nearby observationally dim TGFs. It does not, however, exclude all possible types of nearby observationally dim TGFs. For example, TGFs produced at lower than typical altitudes would appear as radio bright (since radio emissions are not sensitive to altitude) but gamma ray dim (due to atmospheric absorption) events. Also, it is important to note that the peak-finding method outlined in this section rarely locates the pulses directly associated with the NLDN events in question. This means that in many cases the NLDN peak current is not necessarily correlated to any characteristics of the TGF.

The lightning events with peak currents at or below 15 kA are filtered once more so that only those that occurred within 400 km of Fermi's nadir point remain. This requirement was chosen because GBM's TGF detection efficiency is high between 0 and ~400 km distance and drops off rapidly as the distance from Fermi's nadir point increases [*Briggs et al.*, 2013]. Since the purpose of this investigation is to identify TGFs that are classified as dimmer than the count threshold employed by Fermi, this 400 km maximum offset from Fermi's subsatellite point is important because it removes dim events that are only dim because they are far away. Instead, we are left with events that are dim either because they are intrinsically dim or because they are deep in the atmosphere, which is what this study seeks to find.

The LF radio waveform is then analyzed for each of the NLDN events that meets the peak current and subsatellite distance requirements discussed in the previous paragraph. The LF measurements enable us to determine the precise timing of each TGF-like NLDN event at the sensor. By combining this time with the NLDN location, we can determine the precise time at the source location, thus determining the precise arrival time of any NOD-TGF photons at GBM, had it indeed been an NOD-TGF with simultaneous LF radio emissions.

Once LF sferics are found in radio data, they are filtered to differentiate between TGF-like and NBE-like sferics since both are reported as +ICs by NLDN. The +IC and TGF sferics both typically consist of a *series of source pulses* followed by ionospheric reflections. This is different from NBE sferics which have one very fast, high-magnitude source pulse followed by clear ionospheric reflections. While +ICs and TGFs usually last hundreds of microseconds, the typical NBE source pulse lasts tens of microseconds and are relatively easy to distinguish at distances less than 1000 km from the LF sensor. That being said, it is possible that NBEs with sensor-to-NLDN location distances greater than 1000 km were included into the TGF-like candidate data set. This is primarily due to these events' decreasing LF signal-to-noise ratio, leading to a significant decrease in our ability to see NBEs clearly. Examples of NBE-like, TGF-like, and distant (distance source-to-sensor >1000 km) events as they appear in the LF data are shown in Figure 1.

Once the TGF-like discharges are located in the LF data, the events' peaks are found. In this case, we have defined the peak as being the highest-magnitude pulse in the sferic that is within 1.5 ms of the NLDN-reported event time. The peak found using this method is then used to determine the time (in microseconds) that the source pulse reached the sensor. Figure 2 provides an example of this peak-finding process on an actual TGF-like event.

Following this, the NLDN source time is determined by back propagating the TGF-like LF signal to the NLDN-reported source location. We use the source time, an assumed TGF altitude of 13 ± 3 km [*Cummer et al.*, 2011], and Fermi's position (latitude, longitude, and altitude) at the source time to predict what time the gamma rays would have been detected by GBM, had the event produced gamma rays. The time of the TGF is found by correcting the LF radio observation for light travel time from the NLDN source location. Then, using Fermi's location, we calculate the light travel time for the gamma rays to reach Fermi from the TGF source. This gives the time to search the GBM continuous time-tagged gamma ray data for a TGF signal.
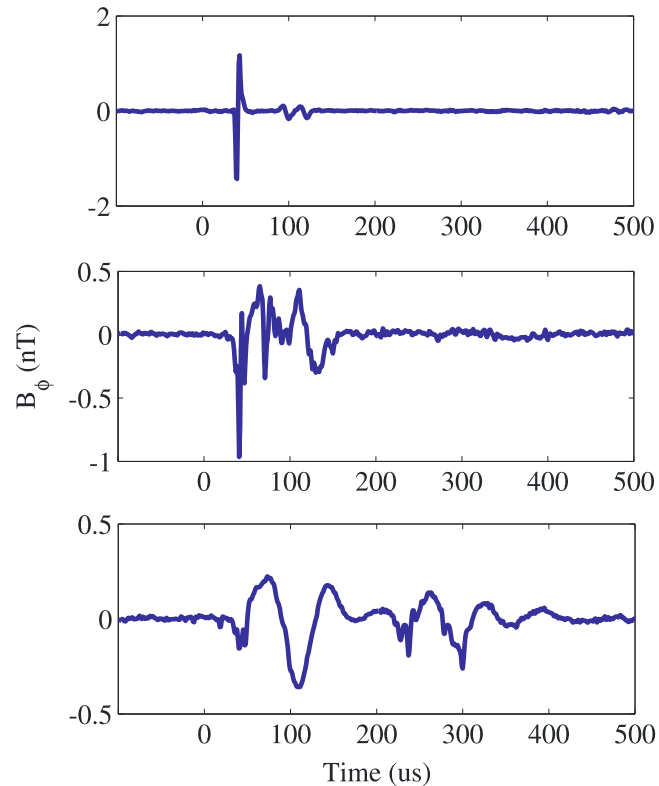
Figure 1. Example of an NBE-like sferic, a TGF-like sferic, and a distant event's sferic in LF data. (top) LF data of an NBE-like event that was 514.4 km from the sensor. (middle) LF data of a TGF-like event detected 477.6 km from the sensor. (bottom) LF data of a distant event located 1029.5 km from the sensor.
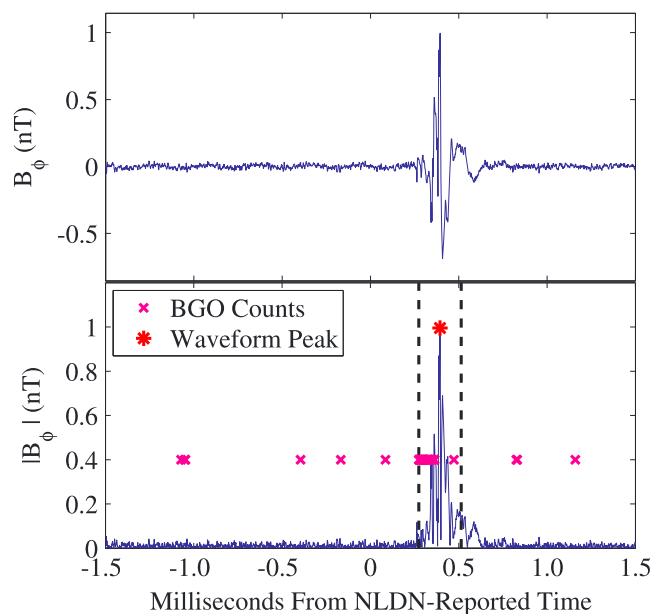
Figure 2. An example of how a reference time is found from the peak of a TGF-like signal. (top) A TGF-like LF waveform limited to within ±1.5 ms of when the NLDN event was expected to arrive at the sensor. (bottom) The peak, marked with an asterisk, is defined as the maximum value of the absolute value of the LF waveform. The total number of counts for this event are the BGO counts that fall within ±100 μs of the peak, windowed with the dashed lines.
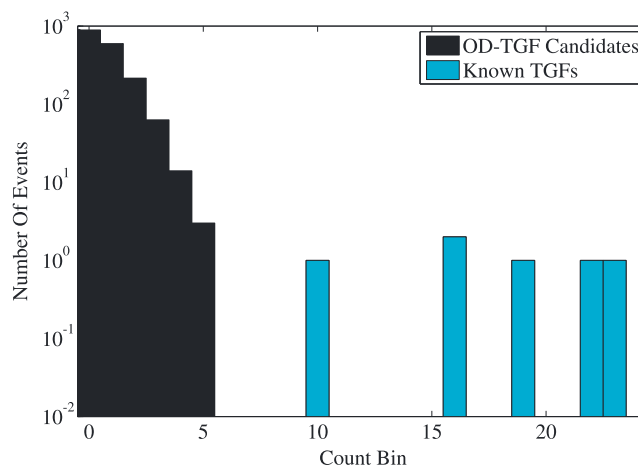
Figure 3. Distribution of photon counts within ±100 μs of GBM peak time. The events at 10, 16, 16, 19, 22, and 23 counts are the six known TGFs found during this search.

According to *Shao et al.* [2010], the source altitude of a TGF can vary anywhere between 10.5 km and 14.1 km; hence, an altitude assumption of 13 ± 3 km is reasonable. *Cummer et al.* [2014] found that the source altitudes of two TGFs were 11.8 ± 0.4 km and 11.9 ± 0.9 km. Considering the uncertainty associated with each of these altitudes, the 13 ± 3 km assumption is still reasonable. The average uncertainty associated with this assumed source altitude is approximately ±10 μs. Once the proposed GBM peak time is calculated, we associate the time with corresponding GBM gamma ray counts from the continuous, time-tagged event data.

4. Results and Analysis

This search yielded 3033 NLDN events that were reported as +ICs and had peak currents ≥15 kA and were within 400 km of Fermi's subsatellite point in the time windows of 29 May 2013 to 5 June 2013, 1 August 2013 to 31 October 2013, and 1 March 2014 to 30 September 2014. Of those 3033 events, 1787 were determined to be TGF-like, and 1246 were classified as being NBE-like based on sferic duration and isolation from other events. Using the timing analysis described in section 3, we thus have for these 1787 events the precise time any photons should have arrived at GBM if the event were a TGF. In the sections below, we statistically analyze these coincident photons (in the form of BGO counts) in several different ways to determine whether there is evidence for a population of weak TGFs within the event set. This process independently identifies some previously known TGFs, proving that it is capable of finding TGFs through a search procedure that does not rely solely on analyzing GBM counts and is thus capable of finding evidence of the existence of nearby dim TGFs (although not necessarily identifies individual nearby dim TGFs) that have simultaneous LF emissions. Interestingly, the statistical evidence favors the conclusion that nearby observationally dim TGFs are rare, as we show below.

4.1. Distribution of BGO Counts Per Lightning Event

We begin by analyzing the BGO counts that are effectively simultaneous with radio emissions when back propagated to the known source location. We define "effectively simultaneous" here as falling within a ±100 μs window centered at the time of peak radio emission amplitude. We chose this window because it was as narrow as possible (to minimize background noise counts) but not so narrow that it excludes TGF counts. After testing various window sizes, 200 μs about the calculated peak time was found to be approximately optimal because it accounts for timing uncertainties in the GBM peak time calculation described in section 3, while still encompassing most, if not all, of each TGF's counts.

Each of the 1787 TGF-like events then yields a total BGO counts per event inside this 200 μs window. The counts-per-event distribution is shown in Figure 3. The most remarkable aspects of this distribution are the six outlying events with ≥10 counts per event (10, 16, 16, 19, 22, and 23). It turns out that these six events are known TGFs that were previously identified through the standard statistical search of GBM data. Fermi identified one other TGF that met the criteria of this search but was not found during this study. This event was not detected using the algorithm outlined in this paper because its sferic was surrounded by stronger
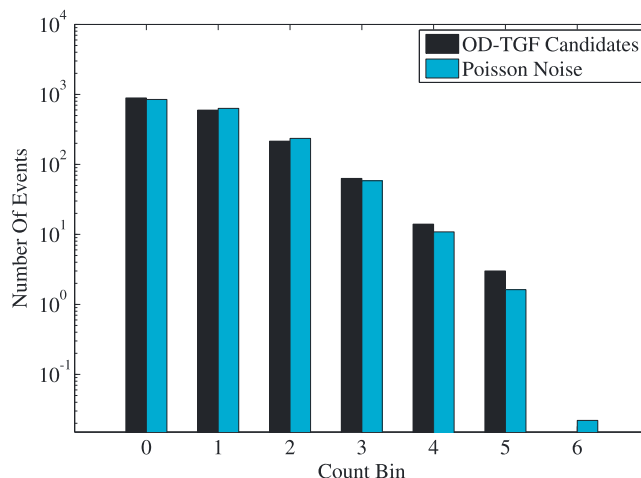
Figure 4. Nearby observationally dim TGF candidate count distribution scaled to counts within 100 µs of selected lightning events (excluding six known TGFs) and background fit Poisson distribution ($\lambda = 0.745$) offset from the lightning events by 2 ms and scaled to expected counts in 200 µs windows.

emissions from other lightning discharges. This resulted in a different lightning sferic's peak being chosen during the peak-finding procedure described in section 3. Although the events we found were already known, we emphasize that our lightning-based search identified them through an approach that imposes no lower threshold on the number of BGO counts. The normal GBM data processing, in contrast, requires at least eight BGO counts to declare a TGF [*Briggs et al.*, 2013]. Since this algorithm is capable of identifying known TGFs associated with above-threshold NLDN events, our approach (which does not use a gamma ray count threshold) is capable of detecting evidence for populations of previously undetected TGFs.

Quantifying the possible presence of nearby dim TGFs requires an analysis of the low end of the counts-per-event distribution to determine whether it is consistent with random noise. We first generate a true background count distribution from the BGO counts recorded 1 to 3 ms before the candidate events—a window 10 times as wide as the window used to generate the candidate distribution. Choosing a time interval close to the expected event time ensures that the noise distributions are as similar as possible.

For ease of analysis, we then fit a Poisson distribution to the background count distribution. It is important to note that GBM does not record a perfect Poisson process as it occasionally detects photons associated with strong cosmic rays. That being said, it is reasonable to compare the background counts to a Poisson distribution in this case, since no cosmic rays were found when the data was time shifted to determine the background count level. The Poisson distribution that best fits the background count rate has a rate parameter $\lambda = 0.745$ events per 200 µs time window and can be compared to the candidate counts-per-event distribution, excluding the six known TGFs, to determine the likelihood of there being nearby dim TGFs.

By visual inspection of the candidate and Poisson distributions in Figure 4, they appear very similar. To determine whether these distributions are statistically indistinguishable from one another, we employ the two sample Anderson-Darling test (AD test) using the following equation from *Pettitt* [1976]:

$$A_{nm}^2 = \frac{1}{nm} \sum_{i=1}^{N-1} \frac{(M_i N - ni)^2}{i(N - i)} \tag{1}$$

where A_{nm}^2 is the AD test statistic, $N = n + m$, the sum of the lengths of each distribution, and M_i is equal to the number of samples in the low-count portion of the candidate distribution less than or equal to the ith smallest in the sorted combination of the candidate and Poisson distributions. According to *Engmann and Cousineau* [2011], the AD test is widely used because of its increased sensitivity toward the tails of the sample distributions and because it is able to detect small variations between two samples better than other popular hypothesis tests. Therefore, we can be sure that this statistic will be sensitive to nearby dim TGFs that may be in the three, four, and five count bins of Figure 3.

We find that $A_{nm}^2 = 0.31$ and that the critical value of this AD statistic at the 95% confidence level (where there is 95% certainty that the two distributions are from different parent distributions) is equal to 2.49. Since
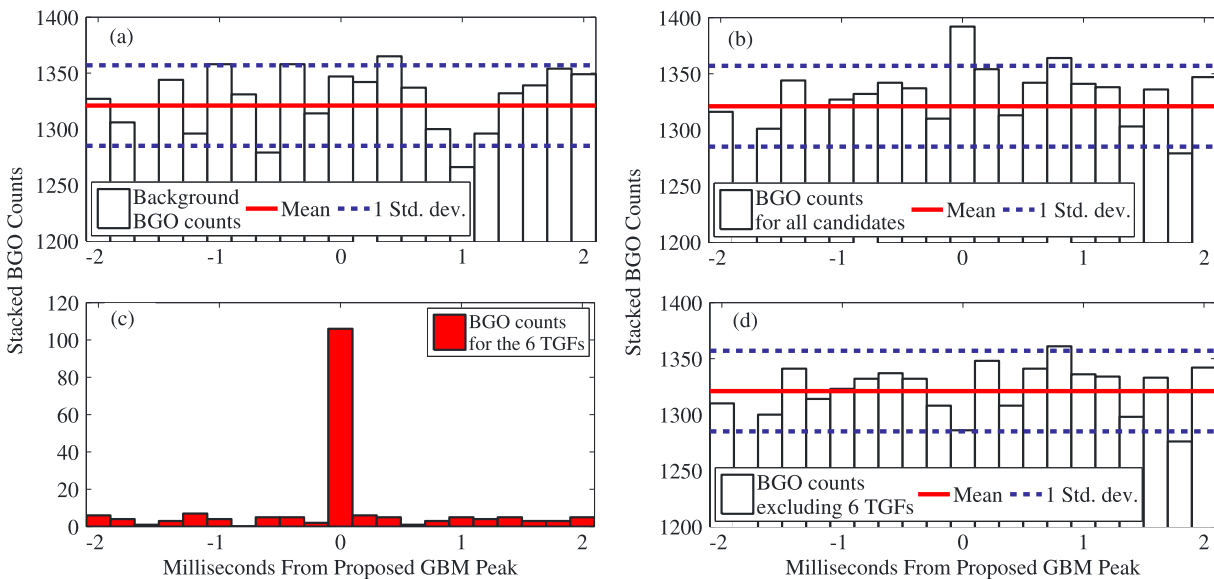
Figure 5. (a) Stacked count distribution of the background counts showing the mean (solid line) and 1 standard deviation from the mean (dashed line). (b) Stacked count distribution of all of the candidates' counts showing the background distribution's mean and standard deviation. (c) Stacked count distribution of the six known TGFs found during the search. (d) Stacked count distribution of the TGF-like events not including the six known TGFs showing the background distribution's mean and standard deviation.

the calculated AD test statistic is well below this critical value we fail to reject the null hypothesis that the candidate and Poisson distributions stem from the same parent distribution.

The results of this AD test show that there is complete statistical consistency between the candidate distribution, excluding the six known TGFs, and the Poisson distribution with rate parameter $\lambda = 0.745$. This implies that the candidate distribution contains no statistically significant nonnoise counts except for those in the six known TGFs. This in turn implies that the observations in Figure 3 contain six TGFs (≥ 10 BGO counts) and may not contain any population of dim TGFs with nine or fewer counts. That there are six bright TGFs and no significant population of dim ones is interesting given that previous work has shown that, down to a cutoff of eight BGO counts, dimmer TGFs are more common [*Tierney et al.*, 2013; *Østgaard et al.*, 2012]. We do address in the section below the possibility that there may be some dim TGF counts in the lower count bins.

4.2. Distribution of BGO Counts in Time

We now examine the distribution of BGO counts for these 1787 candidate events by stacking in time. All BGO counts that were found within ± 2 ms of all of the candidate events were placed into 200 μs bins relative to their expected GBM peak time, and then corresponding bins were summed across all of the candidate events. The purpose of this procedure is to see if a statistically significant excess of gamma rays exists at the center of this plot. As noted in the previous section, a 200 μs bin width was chosen because it encompasses most, if not all, of the candidates' counts (as defined in the peak-finding procedure) and sets them apart from background noise.

The resulting time distribution for all events is shown in Figure 5b. There is an excess of counts above three standard deviations from the background mean within ± 100 μs of the GBM peak time, $t = 0$. However, we can show that this excess is the result of including the six known TGFs that were found in this process. These six known TGFs contributed a total of 106 gamma ray counts to the center bin of Figure 5b, and the time distribution of counts for these six events alone is shown in Figure 5c. With the 106 counts from the six known TGFs removed, there is no significant deviation of the counts in the center bin compared to any other time. Figure 5a shows the distribution of noise-only background counts, which is also the stacked distribution of counts offset by several milliseconds before each candidate event.

Since we easily detect 106 BGO counts in the center bin of Figure 5b, it would be valuable to know the maximum number of BGO counts that could exist in this bin without being a statistically significant excess. To do this, we consider a one-tailed Poisson confidence interval at the 95% confidence level around the mean of the background BGO count rate. By subtracting the mean of the background level from the upper limit of the

Poisson confidence interval, we determine that this maximum number of BGO counts that could accumulate in the center bin of Figure 5b is 60 BGO counts. Note that this number of counts represents only 4.5% of the background count rate's mean.

These 60 counts from hypothetical nearby TGFs would have to be distributed across the one to five count bins in such a way that they remain statistically indistinguishable from the background noise in Figure 4. As such their count distribution would have to roughly follow a Poisson shape, with mostly one- and two-count hypothetical TGFs and only a few with four and five counts, yielding 28 hypothetically possible TGFs. This analysis shows that if a population of nearby dim TGFs collectively producing more than approximately one half of the gamma rays of the six detected TGFs existed, we would have detected the population via the time stacking analysis.

In the analysis that follows, we use the results shown thus far and consider two distinct assumptions, each of which is statistically consistent with the data: (1) that there could be no observed TGF counts except for the six known TGFs and (2) that there could be as many as 60 BGO counts from nearby dim TGFs in the low-count bins in addition to the six known TGFs in this distribution. These are essentially the lower and upper bounds, respectively, on the number of TGF counts that could be in the low-count bins (five and lower) in Figure 4. We explore below what this means for the overall rate of TGFs as well as the implications of the distribution of TGF brightness.

4.3. Probability of TGF Occurrence

We have shown that in this set of 1787 NLDN-reported IC lightning events, there are at least six TGFs and as many as approximately 34 TGFs (28 dim TGFs from the upper bound of 60 BGO counts plus six known TGFs). This is a large enough sample that we can reliably use to bound the answer to the following question: given an NLDN report of a +IC lightning event with peak current ≥15 kA whose emitted LF waveform is consistent with it, having been produced during early stage IC leader development, what is the probability that a TGF occurred at the time of the peak LF radio emission at a source altitude of 13 ± 3 km?

The range of probabilities consistent with the observations is calculated using the normal approximation of the binomial confidence interval [*Agresti*, 2007] at the 95% confidence level, which is defined as

$$P = p \pm z\sqrt{\frac{1}{n}p(1-p)} \tag{2}$$

where p is the central probability of there being a TGF in this distribution, z is the $1 - \frac{1}{2}\alpha$ percentile, which at the 95% confidence level is equal to 1.96, and n is the number of events in the sample or 1787 in this case. If we base the TGF/lightning limits on the observed number of TGFs, then the central probability is $\frac{6}{1787}$ with lower and upper bounds of $\frac{1}{500}$ and $\frac{1}{210}$. If instead we base the limits on the upper limit of the number of TGFs allowed by the gamma ray observations, then the central probability is $\frac{34}{1787}$ with lower and upper bounds of $\frac{1}{80}$ and $\frac{1}{40}$, respectively. These intervals are lower bounds on the total TGF rate because they are based only on TGFs that are associated with lightning events that meet our constraints.

We can now extrapolate this number to estimate the global TGF rate. We assume that 75% of all lightning is in-cloud [*Rakov and Uman*, 2003; *Boccippio et al.*, 2001] so that the estimates calculated by *Briggs et al.* [2013] and *Smith et al.* [2011a, 2011b] can be recalculated to only account for in-cloud flashes. We find that the fraction of NLDN +IC events that exceed our 15 kA threshold is approximately 15%, and accounting for lower detection efficiency of weaker events, we estimate using NLDN that this fraction is actually 10%. Assuming that 10% can be extrapolated to global statistics, the worldwide rate of IC lightning flashes per day of 3.8 million [*Christian et al.*, 2003] implies 380,000 IC flashes per day that meet our peak current constraints.

The probability range associated with there being only six TGFs in this distribution found using equation (2) is applied to the total number of IC lightning flashes per day that are ≥15 kA and is converted to provide the range of TGFs that occur per day worldwide, N_{TGF}, and becomes $760 \leq N_{TGF} \leq 1810$. This is the estimate of the global number of TGFs per day that occur under the conditions of our analysis and thus should be considered a lower bound on the total TGF rate. This range is consistent with the estimates made by *Briggs et al.* [2013], *Tierney et al.* [2013], *Carlson et al.* [2011], and *Smith et al.* [2011a, 2011b], which all estimated N_{TGF} to fall within the range above. The probability range associated with there being approximately 34 TGFs, accounting for the possibility of some nearby observationally dim TGF counts, is used in the same fashion to estimate the range of N_{TGF} and becomes $4750 \leq N_{TGF} \leq 9500$.
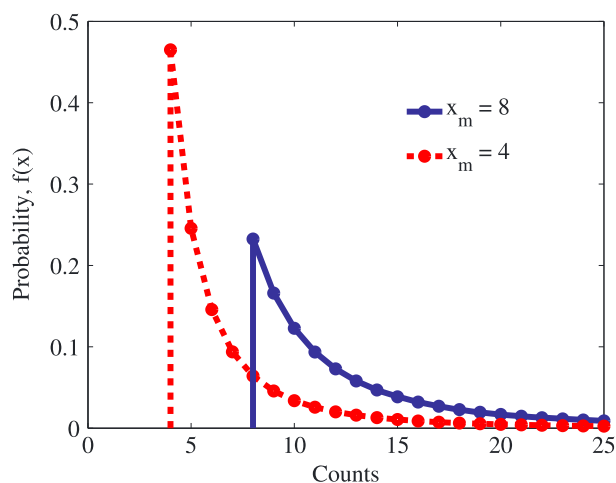
Figure 6. The power law pdfs ($\alpha = 2.86$) with $x_m = 4$ and $x_m = 8$. Notice that the lower cutoff pdf yields lower probabilities of observing higher photon events than the eight photon cutoff pdf.

4.4. Implications for the Power Law Distribution of TGF Brightness

Because our TGF search procedure has no inherent lower count threshold, we have the ability to assess whether the power law distributions of TGF brightness extend below the count threshold of prior TGF searches (for example, the eight BGO count threshold used by GBM [*Briggs et al.*, 2013; *Tierney et al.*, 2013]). All power law probability distributions must have some form of lower cutoff so that they remain integrable, and where this cutoff is has significant implications for both TGF physics and for estimates of the global TGF rate. For example, *Østgaard et al.* [2012] extrapolated a TGF rate based on lowering this cutoff by assuming a lower detection threshold of RHESSI using ADELE observations.

Recall that our threshold-free search revealed six TGFs with 10 or more BGO counts and no events at all with six to nine counts. This particular observation is expected to be a random realization of the power law distribution of TGF fluence found by *Tierney et al.* [2013], which has an exponent of $\alpha = 2.86$ for BGO counts that are uncorrected for instrumental effects. Intuitively, it seems unlikely that a draw of six events from a distribution with this fairly steep exponent and with a low cutoff (say two BGO counts) would result in six events above 10 counts and none between six and nine, but the consistency of this observation with a specific probability distribution can be quantified, and we do so through the following assumptions and procedure. As in section 4.3, we separately consider the cases of no TGF counts in the low-count bins (the lower bound) and 60 TGF counts in the low-count bins (the upper bound).

4.4.1. Lower Bound Case

We start with the lower bound case of no TGF counts other than the six identified TGFs. This indicates that BGO counts associated with the remaining 1781 events we found were consistent with noise and is supported by our analysis that showed the strong statistical consistency of these counts with Poisson noise. We assume that the true TGF fluence distribution is a power law with a sharp cutoff at an unknown BGO count level. This cutoff must be below eight based on prior observations [*Briggs et al.*, 2013; *Tierney et al.*, 2013], but there is no information until now about where it might be below that. Third, we begin with a baseline power law exponent of $\alpha = 2.86$ because the BGO counts we are using are not corrected for instrumental effects [*Tierney et al.*, 2013], although we consider smaller exponents as well. The resulting family of power law probability density functions (pdfs) that involve a lower cutoff threshold x_m and the power law parameter α are defined by

$$f(x) = \begin{cases} \frac{\alpha-1}{x_m} \left(\frac{x}{x_m} \right)^{-\alpha} & \text{for } x \geq x_m, \\ 0 & \text{otherwise} \end{cases} \tag{3}$$

Note that this distribution is continuous everywhere except x_m but will yield results nearly identical to the same procedure done with a discrete distribution. Figure 6 illustrates how this power law pdf changes when the lower cutoff is changed from eight counts to four counts. From this figure it is clear that higher count events, and thus our observation of six high-count TGFs, will be less probable when the cutoff is lowered.
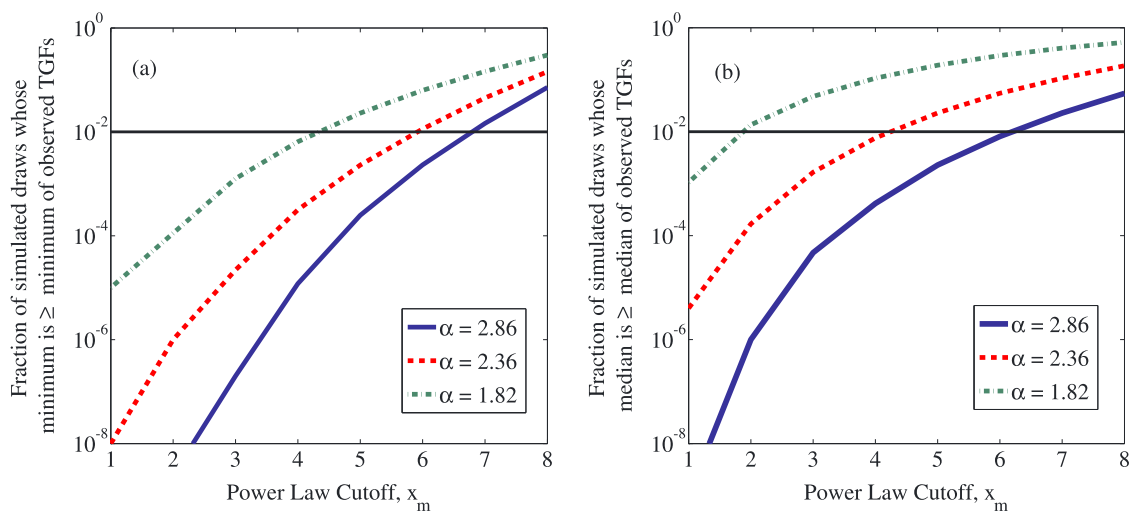
Figure 7. The results of the Monte Carlo simulations (a) comparing the smallest (minimum) count of a simulated sample of six TGFs to the smallest (minimum) of the observation of six known TGFs and (b) comparing the median count of a simulated sample of six TGFs to the median of the observation of six known TGFs. In each plot, the three curves represent the probability of observing a TGF with different indices of the power law as a function of cutoff. The horizontal line represents each curve's intersection with 1% probability.

We quantify this probability through the following question: given a power law distribution of known cutoff x_m and exponent α, what is the probability that the minimum count of six draws from the TGF fluence distribution is equal to or greater than 10 BGO counts, the minimum count of the six TGFs we observed? With only six TGFs to analyze we are limited in the statistical approaches we can apply to answer this question. The approach described below is simple and provides quantitative insight into how consistent our observations are with a particular cutoff.

A Monte Carlo simulation was adopted as the method of choice for determining the distribution of the smallest count observed of six draws from power law distributions with cutoffs that vary from one through eight counts. One draw is a randomly generated representation of the total counts associated with a particular simulated event. We draw 6 times from each power law with varying cutoff, because we are simulating the observation of the six TGFs we found in Figure 3 to see how consistent the simulations are to our actual observation. This simulation was run 1×10^9 times.

We then compute the fraction of draws for which the smallest count of the simulated sample was greater than or equal to the smallest count of the observation. If this fraction is relatively large, then our observations are consistent with that power law; but if the fraction is small, then the likelihood of our observations given the assumed distribution is low. This computation is done using three different power law exponents: the baseline $\alpha = 2.86$ that is not corrected for GBM instrumental effects [*Tierney et al.*, 2013], $\alpha = 2.36$, which is an arbitrarily chosen exponent that allows for the possibility that the distribution of TGFs detected with our approach might be more consistent with a lack of low-count TGFs, and $\alpha = 1.82$ [*Albrechtsen*, 2015], which accounts for the possibility of a lower exponent at low counts [*Østgaard et al.*, 2012]. These three cases bound the range of TGF count power law distributions reported in literature. The baseline exponent ($\alpha = 2.86$) should not be confused with the exponents found for instrumental effect-corrected counts [*Østgaard et al.*, 2012; *Tierney et al.*, 2013; *Marisaldi et al.*, 2014].

Figure 7a shows the fraction of events that meet or exceed the observed minimum of 10 counts as a function of power law cutoff x_m. We first consider the fraction for the observed power law exponent $\alpha = 2.86$. As expected, the observation of only high-count TGFs becomes less and less likely as the power law cutoff decreases. The observations are very unlikely (less than 10^{-8} probability) for $x_m = 1$, and consequently, we can assert that the observations strongly favor a power law fluence distribution that does not extend to very low BGO count TGFs. Equivalently, the observations suggest that weak TGFs are much more rare than would be expected by simple extension of the known power law to low fluences.

Using 1% as the level of acceptable statistical consistency between the observations and a given model, we find that the data are consistent with a cutoff x_m of about 6.7 or higher for the known power law exponent

$\alpha = 2.86$. It seems an interesting coincidence that this analysis favors a cutoff very close to that which has been assumed in the standard GBM analysis [*Briggs et al.*, 2013] — perhaps the development of that analysis, testing to avoid contamination of the TGF sample, reached the lowest possible threshold. We emphasize, however, that our analysis uses no cutoff or threshold and arrived at this number independently. A larger event sample would certainly be useful to firm up these numbers, but the conclusion remains that this analysis indicates that weak TGFs are uncommon.

In addition, we also acknowledge the possibility that the required association with NLDN-detected lightning events means that our search procedure samples a subset of TGFs that could have a different power law exponent. Consequently, Figure 7a also shows the same dependence of the fraction of simulations that meet or exceed the observed minimum count for lower power law exponents ($\alpha = 2.36$ and $\alpha = 1.82$) that would make high-count TGFs more likely. A significant drop in the exponent to 2.36 would not change the fundamental conclusion, namely, that our actual observations are consistent with a cutoff in the power law distribution that is not much lower than the eight count threshold used in the standard GBM search. This cutoff drops from 6.7 to 5.9 BGO counts, but it still implies that weak TGFs are uncommon. Similarly, if the exponent is dropped further ($\alpha = 1.82$), we also see that there is a cutoff above one count. We thus assert that our fundamental conclusion, namely, that weak TGFs are rarer than implied by a simple extension of the power law to low counts, is robust to uncertainty in the exponent of the power law distribution. The apparent cutoff found during this analysis of 6.7 counts corresponds to a TGF photon fluence at satellite altitudes of 0.042 photons/cm^2 when the BGO effective area is 160 cm^2 [*Briggs et al.*, 2013].

To test our results using a second statistic, we also used a Monte Carlo simulation that compares the median count of six draws from power law distributions with cutoffs that vary from one to eight counts to the median of our actual observation of six TGFs. Figure 7b shows that our observation is consistent with a power law cutoff, x_m, of six or more BGO counts when $\alpha = 2.86$ and also shows results consistent with the Monte Carlo simulation described in the previous paragraphs when a lower power law exponent is used. This shows that our observations favor a power law fluence distribution that does not extend to low BGO counts. It is also consistent with our previous conclusions stating that this analysis favors a power law cutoff close to what is already used in the standard GBM analysis [*Briggs et al.*, 2013] and that nearby observationally dim TGFs are uncommon. The cutoff found using the Monte Carlo simulation described in this paragraph corresponds to a TGF photon fluence at satellite altitudes equal to 0.038 photons/cm^2 when a BGO effective area of 160 cm^2 is assumed [*Briggs et al.*, 2013].

4.4.2. Upper Bound Case

We now consider the case where there may be as many as 60 low fluence TGF counts in the noise portion of the count distribution in Figure 4 (recall that this is an upper bound based on the time-stacking analysis in section 4.2). The minimum- and median-based statistical tests will no longer be applicable to this case because we are allowing the existence of some low-count TGFs. We thus take a different approach. First, we recognize that the assumed presence of low-fluence TGF counts implies that they must be spread over all of the bins in Figure 4, as there is no way to distribute 60 counts in (for example) just the four and five count bins of Figure 4 without changing the consistency with a Poisson distribution. We thus assume that a power law that encompasses these possible 60 TGF counts must extend down to one count and cannot have a sharp cutoff.

We next establish an observation and the statistical consequences of that observation. This data set contains 106 BGO counts from known TGFs in the 10 and higher count bins. Given that observation, we can then ask how likely it is to observe 60 or fewer BGO counts in the five and lower count bins for an assumed statistical distribution. As in the lower bound case, we first assume a power law exponent of 2.86 that extends down to one count and use a Monte Carlo simulation (1 million realizations) to estimate the fraction of realizations that contain 60 or fewer counts in the lower bins (at and below the five count bin) given 106 counts in the higher bins (10 and above). Inspection suggests that 60 is far too few counts to be consistent with a power law of this steepness. The Monte Carlo simulation confirms this, finding that this occurs with probability 7.9×10^{-5}, far below a consistency threshold of 0.01. Thus, even the maximum possible number of low-fluence TGF counts is too few to be consistent with an $\alpha = 2.86$ power law that extends down to low fluence.

We repeated the calculation for the same lower power law exponents as in the lower bound case. For $\alpha = 2.36$, sufficiently few low-fluence counts were observed with probability 7.5×10^{-4}, which is still significantly below a consistency threshold of 0.01. For $\alpha = 1.82$, we obtain a probability of 0.0102 and thus cannot rule out the consistency of this distribution with the observations. However, it is important to realize that this power law is

assumed to hold over the entire TGF fluence range and thus is far more likely to produce high-fluence events than the experimentally measured power law exponent of 2.86 that applies above eight BGO detector counts. Thus, even a distribution that has a 2.86 exponent above eight counts and a 1.82 exponent below eight counts is not consistent with the upper bound of 60 low fluence BGO counts.

Consequently, we can conclude that our observations, which are fundamentally unbiased with respect to BGO counts (except for those introduced by the 15 kA threshold), are statistically inconsistent with a power law distribution that extends all the way to lower observed TGF fluence. Thus, even accounting for the possibility of low-fluence TGF counts in our data set, we find that nearby observationally dim TGFs may be rarer than predicted by measured power law distributions.

5. Summary and Conclusions

Using a targeted NLDN-based search, we have developed and demonstrated a lightning-based TGF search procedure that is able to find TGFs with no explicit lower threshold on the number of photons or counts. This search approach is, in principle, able to identify a population of weak TGFs that are below the thresholds of prior photon-based searches. Out of 1787 total TGF candidate events accumulated over an 11 month period, this search procedure independently identified six known TGFs, all with 10 or more BGO counts in 200 μs search windows defined by the associated radio emissions. This establishes the basic validity of the approach and its ability to identify TGFs without any assumed lower fluence threshold.

We found that identifying low-count TGFs is limited to some degree by background noise counts. Several different analysis approaches were used to establish bounds on the number of counts from low-fluence (five and lower counts per 200 μs time window, where the background noise is nonnegligible) TGFs that could be present in our data set. The statistical consistency of the low fluence distribution with a Poisson distribution implies that there could be as few as no low-fluence TGF counts, while a time-stacking procedure shows that, at the 95% confidence level, there are no more than 60 low-fluence TGF counts in that distribution.

Using these upper and lower bounds on the number of detector counts that could come from nearby observationally dim TGFs, we calculated statistical bounds on the fraction of lightning events meeting our search criteria that produce TGFs. Assuming that the six known TGFs are the only TGFs found using this search, we find that the 95% confidence interval for the probability of TGF occurrence, given a lightning event meeting our criteria, is $\frac{1}{500}$ to $\frac{1}{210}$. This range corresponds to 760 to 1810 TGFs occurring per day worldwide and agrees with the estimates made by *Briggs et al.* [2013], *Tierney et al.* [2013], *Carlson et al.* [2011], and *Smith et al.* [2011a, 2011b]. If we allow that there are as many as 60 additional TGF counts, corresponding to 28 low-count TGFs, then the 95% confidence interval changes to $\frac{1}{80}$ to $\frac{1}{40}$, which corresponds to between approximately 4750 and 9500 TGFs occurring per day worldwide.

Although our search did not yield nearly enough TGFs to define the TGF fluence distribution across all possible values, it does provide enough TGF observations to statistically test the consistency of different fluence distributions with our data. We again performed this analysis separately for the lower and upper bounds on the number of low-fluence TGF counts in our data set. First, assuming that there were zero low-fluence TGF counts in our data, we used a Monte Carlo simulation to evaluate the likelihood of the smallest count of the six known TGFs found during this search assuming a power law pdf with sharp cutoffs ranging from 1 to 8 counts. Using the known power law exponent for GBM counts of $\alpha = 2.86$, we found at the 99% confidence level (probability threshold 1%) that the observations are consistent with a cutoff of approximately 6.7 counts, which corresponds to a TGF fluence equal to 0.042 photons/cm^2. This implies that TGFs at lower than eight counts are significantly rarer than expected by extrapolation of the known power law exponent to lower count events. We performed the same test with lower power law exponents, and in all cases the data favor a cutoff that implies that nearby observationally dim TGFs are rarer than expected.

We next allowed that there could be as many as 60 counts from dim TGFs hiding in the background noise distribution. Given the observation of 106 counts from TGFs with fluence of 10 and higher BGO counts, we assessed (again with a Monte Carlo simulation) the likelihood of observing 60 or fewer counts from low fluence TGFs under that constraint. For the known power law exponent $\alpha = 2.86$ and also smaller values, it is very unlikely that as few as 60 low-fluence TGF counts would be observed given 106 high-fluence TGF counts. Thus, even allowing for the possibility of low-fluence TGF counts in our data, the observations statistically favor the conclusion that low-fluence TGFs are significantly rarer than is expected from extrapolation of the known power law fluence distribution for high-fluence TGFs.

In conclusion, in an attempt to paint a clearer picture of TGF occurrence rate and fluence distribution, we searched for nearby observationally dim TGFs using a radio-guided approach that incorporates no lower limit on TGF fluence. This search for NOD-TGFs independently found several known TGFs, but found no individually identifiable and previously unknown TGFs. A statistical analysis of the resulting count distribution using two distinct approaches favors the conclusion that low-fluence TGFs are rarer than predicted by extrapolation to low fluence of known power laws. One of many resulting possibilities is that TGFs may have a lower intrinsic brightness threshold. That being said, a larger number of events (greater than 1787) is needed to increase the statistical certainty of these results. As such, this research is ongoing for the purposes of increasing the event sample size.

References

Agresti, A. (2007), Confidence intervals for a binomial proportion, in *An Introduction to Categorical Data Analysis, in Statistical Inference For Binomial Parameters*, p. 9, John Wiley, New Jersey.

Albrechtsen, K. H. (2015), Search for unidentified terrestrial gamma-ray flashes, MS thesis, 110 pp., Univ. of Bergen, Bergen, Norway.

Boccippio, D. J., K. L. Cummings, H. J. Christian, and S. J. Goodman (2001), Combined satellite- and surface-based estimation of the intra-cloud-cloud-to-ground lightning ratio over the continental United States, *Mon. Weather Rev.*, 129(1), 108–122, doi:10.1175/1520-0493(2001)129.

Briggs, M. S., et al. (2013), Terrestrial gamma-ray flashes in the Fermi era: Improved observations and analysis methods, *J. Geophys. Res. Space Physics*, 118, 3805–3830, doi:10.1002/jgra.50205.

Carlson, B. E., N. G. Lehtinen, and U. S. Inan (2010), Terrestrial gamma ray flash production by active lightning leader channels, *J. Geophys. Res.*, 115, A10324, doi:10.1029/2010JA015647.

Carlson, B. E., T. Gjesteland, and N. Østgaard (2011), Terrestrial gamma-ray flash electron beam geometry, fluence, and detection frequency, *J. Geophys. Res.*, 116, A11217, doi:10.1029/2011JA016812.

Carlson, B. E., T. Gjesteland, and N. Østgaard (2012), Connecting the terrestrial gamma-ray flash source strength and observed fluence distributions, *J. Geophys. Res.*, 117, A01314, doi:10.1029/2011JA017122.

Celestin, S., and V. P. Pasko (2011), Energy and fluxes of thermal runaway electrons produced by exponential growth of streamers during the stepping of lightning leaders and in transient luminous events, *J. Geophys. Res.*, 116, A03315, doi:10.1029/2010JA016260.

Chanrion, O., and T. Neubert (2010), Production of runaway electrons by negative streamer discharges, *J. Geophys. Res.*, 115, A00E32, doi:10.1029/2009JA014774.

Christian, H. J., et al. (2003), Global frequency and distribution of lightning as observed from space by the Optical Transient Detector, *J. Gephys. Res.*, 108(D1), 4005, doi:10.1029/2002JD002347.

Connaughton, V., et al. (2010), Associations between Fermi Gamma-ray Burst Monitor terrestrial gamma-ray flashes and sferics from the World Wide Lightning Location Network, *J. Geophys. Res.*, 115, A12307, doi:10.1029/2010JA015681.

Cummer, S. A., G. Lu, M. S. Briggs, V. Connaughton, S. Xiong, G. J. Fishman, and J. R. Dwyer (2011), The lightning-TGF relationship on microsecond timescales, *Geophys. Res. Lett.*, 38, L14810, doi:10.1029/2011GL048099.

Cummer, S. A., M. S. Briggs, J. R. Dwyer, S. Xiong, V. Connaughton, G. J. Fishman, G. Lu, F. Lyu, and R. Solanki (2014), The source altitude, electric current, and intrinsic brightness of terrestrial gamma ray flashes, *Geophys. Res. Lett.*, 41, 8586–8593, doi:10.1002/2014GL062196.

Cummins, K., and M. J. Murphy (2009), An overview of lightning locating systems: History techniques, and data uses, with an in-depth look at the U.S. NLDN, *IEEE Trans. Electromagn. Compat.*, 51, 499–518.

Cummins, K., M. J. Murphy, E. A. Bardo, W. L. Hiscox, R. Pyle, and A. E. Pifer (1998), A combined TOA/MDF technology upgrade of the U.S. National Lightning Detection Network, *J. Geophys. Res.*, 103, 9035–9044, doi:10.1029/98JD00153.

Dwyer, J. R. (2003), A fundamental limit on electric fields in air, *Geophys. Res. Lett.*, 30(20), 2055, doi:10.1029/2003GL017781.

Dwyer, J. R. (2004), Implications of X-ray emission from lightning, *Geophys. Res. Lett.*, 31, L12102, doi:10.1029/2004BL019795.

Dwyer, J. R. (2007), Relativistic breakdown in planetary atmospheres, *Phys. Plasmas*, 14, 42901, doi:10.1063/1.2709652.

Dwyer, J. R. (2008), Source mechanisms of terrestrial gamma-ray flashes, *J. Geophys. Res.*, 113, D10103, doi:10.1029/2007JD009248.

Dwyer, J. R., and S. A. Cummer (2013), Radio emissions from terrestrial gamma-ray flashes, *J. Geophys. Res. Space Physics*, 118, 3769–3790, doi:10.1002/jgra.50188.

Engmann, S., and D. Cousineau (2011), Comparing distributions: The two-sample Anderson-Darling test as an alternative to the Kolmogorov-Smirnoff test, *J. Appl. Quant. Methods*, 6(3), 1–17.

Fishman, G. J., et al. (1994), Discovery of intense gamma-ray flashes of atmospheric origin, *Science*, 264, 1313–1316, doi:10.1126/science.264.5163.1313.

Fuschino, F., et al. (2011), High spatial resolution correlation of AGILE TGFs and global lightning activity above the equatorial belt, *Geophys. Res. Lett.*, 38, L14806, doi:10.1029/2011GL047817.

Gurevich, A., G. M. Milikh, and R. Roussel-Dupre (1992), Runaway electron mechanism of air breakdown and preconditioning during a thunderstorm, *Phys. Lett. A*, 165, 463–468.

Lu, G., R. J. Blakeslee, J. Li, D. M. Smith, X.-M. Shao, E. W. McCaul, D. E. Buechler, H. J. Christian, J. M. Hall, and S. A. Cummer (2010), Lightning mapping observation of a terrestrial gamma-ray flash, *Geophys. Res. Lett.*, 37, L11806, doi:10.1029/ 2010GL043494.

Lu, G., S. A. Cummer, J. Li, F. Han, D. M. Smith, and B. W. Grefenstette (2011), Characteristics of broadband lightning emissions associated with terrestrial gamma ray flashes, *J. Geophys. Res.*, 116, A03316, doi:10.1029/2010JA016141.

Marisaldi, M., F. Fuschino, and M. Tavani (2014), Properties of terrestrial gamma ray flashes detected by AGILE MCAL below 30 MeV, *J. Geophys. Res. Space Physics*, 119, 1337–1355, doi:10.1002/2013JA019301.

Moss, G., V. Pasko, N. Liu, and G. Veronis (2006), Monte Carlo model for analysis of thermal runaway electrons in streamer tips in transient luminous events and streamer zones of lightning leaders, *J. Geophys. Res.*, 111, A02307, doi:10.1029/2005JA011350.

Østgaard, N., et al. (2012), The true fluence distribution of terrestrial gamma flashes at satellite altitude, *J. Geophys. Res.*, 117, A03327, doi:10.1029/2011JA017365.

Pettitt, A. N. (1976), A two-sample Anderson-Darling rank statistic, *Biometrika*, 63(1), 161–168.

Rakov, V. A., and M. A. Uman (2003), Lightning Physics and Effects, in *Incidence of Lightning*, pp. 24–52, Cambridge Univ. Press, New York.

Shao, X.-M., T. Hamlin, and D. M. Smith (2010), A closer examination of terrestrial gamma-ray flash-related lightning processes, *J. Geophys. Res.*, 115, A00E30, doi:10.1029/2009JA014835.

Smith, D. M., et al. (2011a), A terrestrial gamma ray flash observed from an aircraft, *J. Geophys. Res.*, *116*, D20124, doi:10.1029/2011JD016252.

Smith, D. M., et al. (2011b), The rarity of terrestrial gamma-ray flashes, *Geophys. Res. Lett.*, *38*, L08807, doi:10.1029/2011GL046875.

Stanley, M. A., X.-M. Shao, D. M. Smith, L. I. Lopez, M. B. Pongratz, J. D. Harlin, M. Stock, and A. Regan (2006), A link between terrestrial gamma-ray flashes and intracloud lightning discharges, *Geophys. Res. Lett.*, *33*, L06803, doi:10.1029/2005GL025537.

Tierney, D., et al. (2013), Fluence distribution of terrestrial gamma ray flashes observed by the Fermi Gamma-ray Burst Monitor, *J. Geophys. Res. Space Physics*, *118*, 6644–6650, doi:10.1002/jgra.50580.

Wilson, C. T. R. (1925), The acceleration of beta-particles in strong electric fields such as those of thunderclouds, *Proc. Cambridge Phil. Soc.*, *22*, 534–538, doi:10.1029/S0305004100003236.